Title
n-p INTERACTION AT 3.7 BeV

Authors
Goldhaber, Sulamith
Goldhaber, Gerson
Shen, Benjamin C.
et al.

Publication Date
1964-07-01

University of California

Ernest O. Lawrence Radiation Laboratory

Berkeley, California

(To be presented at the 1964 International Conference on High Energy Physics, Dubna, U.S.S.R. - August 5-15, 1964)

UCRL-11464

UNIVERSITY OF CALIFORNIA

Lawrence Radiation Laboratory
Berkeley, California

Contract No. W-7405-eng-48

$\pi^- p$ INTERACTION AT 3.7 BEV

Sulamith Goldhaber, Gerson Goldhaber, Benjamin C. Shen, and George H. Trilling

(Presented by Sulamith Goldhaber)

July 16, 1964

$\pi^- p$ INTERACTION AT 3.7 BEV*

Sulamith Goldhaber, Gerson Goldhaber, Benjamin C. Shen, and George H. Trilling
Lawrence Radiation Laboratory and Department of Physics
University of California, Berkeley, California

(Presented by Sulamith Goldhaber)

July 16, 1964

Asymmetry in the decay angular distribution of the neutral ρ has been observed by a number of investigators in reactions leading to three particles in the final state $\pi^- + p \rightarrow \pi^- + \pi^+ + n$. This phenomenon has been attributed to either interference of the resonating p-wave of the $(\pi^+\pi^-)$ system with other angular momenta (i.e., s- and d-waves) present in the background or to a scalar singlet $(\pi^+\pi^-)$ resonance unresolved from the vector ρ meson.[1]

We find a similar asymmetry in the decay angular distribution of the neutral ρ formed in a four-particle reaction $\pi^- + p \rightarrow \pi^+ + \pi^- + p + \pi^-$. We propose that the major part of the asymmetry which we observe is due to the presence of the N^{*++} isobar overlapping the ρ resonance. We further give evidence that the 3,3 resonance comes in part from the decay of a $p\pi^+\pi^-$ state. Comparing the peak, we observe in the $p\pi^+\pi^-$ mass distributions with the inelastic pπ cross section obtained by counter techniques, we conclude that our data could be associated with the $N^*_{1/2}(1510)$ isobar.[2] The width of the mass peak we observe Γ = 240 MeV is considerably larger than the $N^*(1510)$ resonance. The large width may be due to the presence of additional structure in the T = 1/2 and T = 3/2 isotopic spin states as observed in πp scattering experiments.

* Work sponsored by the U. S. Atomic Energy Commission.

The data discussed here come from an experiment carried out in a momentum analyzed negative beam of the Lawrence Radiation Laboratory's Bevatron using the 72-inch hydrogen bubble chamber as detector. The reaction we will disucss here is one leading to four charged particles in the final state, viz. $\pi^- p \rightarrow \pi^- \pi^+ p \pi^-$. The kinematic fitting and ionization information reduces the number of events with ambiguous interpretation to less than 1%. The measurements of all events produced in the $\pi^- p$ interaction have been carried out with the "flying spot digitizer" (FSD) of the Lawrence Radiation Laboratory.

We find that only 5% (1129 events) of $\pi^- p$ interactions at 3.7 BeV/c give four charged particles in the final state. This leads to a cross section of 1.8 ± 0.4 mb for this reaction. Two-thirds of the events leading to a four-particle final state are the decay product of resonances. We list all the channels feeding the four-particle final state in Table I. It is interesting at this point to compare the data with similar data obtained in the $\pi^+ p$ interaction. The cross section for the four-particle state in the $\pi^+ p$ interaction is about a factor of three higher. The lack of the strong $\rho^o N^{*++}$ channel suppresses the cross section in the $\pi^- p$ interaction. On the other hand, the non-resonating channel is roughly of the same intensity in the two reactions.

In Fig. 1 we show the mass distributions of the three two-particle final states, i.e., $(\pi^+\pi^-)$, $(p\pi^+)$, and $(p\pi^-)$. Since two π^- mesons are present we show the invariant masses formed by both combinations. The formation of both the ρ^o and N^{*++} is evident. The N^{*o} formation is seen much more clearly when we confine ourselves to events in the double resonance region, i.e., together with the ρ^o

meson, as shown in Fig. 2; the shaded part gives the mass distribution for events with four momentum transfer to the ρ^o, $\Delta^2(\rho^o) < 50\ m_\pi^2$. We find three distinct peaks with central values 1220, 1480, 1690 MeV and respective full width at half maximum of 120, 120, 100 MeV. These we interpret as the $N^{*o}_{3/2}(1238)$, $N^{*o}_{1/2}(1510)$, and $N^{*o}_{1/2}(1688)$ isobars respectively.

A scatter plot of the $(\pi^+\pi^-)$ mass versus the $(p\pi^+)$ mass (two points for each event, see Fig. 3) shows that there exists a large overlap region between the N^{*++} and ρ^o resonances. By plotting a density distribution of the two resonance bands we obtain an estimate of the total $N^{*++}_{3/2}$ isobar production (see Table I). The overlap of the two resonance bands has a crucial effect on the decay angular distribution of the ρ meson. Confining ourselves to events with small momentum transfer to the $p\pi^-$ system, we would expect on the one pion exchange model (see Fig. 4a) the scattering amplitude $P_1^o = \cos\alpha$ to dominate since the ρ meson can be identified with a scattering vertex of two pions in the p-state. We find instead of the expected $\cos^2\alpha$ angular distribution, a strongly asymmetric one (see Fig. 5). The solid curve shown is an expansion in $\cos\alpha$ viz.: $I(\alpha) = A + B\cos\alpha + C\cos^2\alpha$. The coefficients are $B/A = 1.5 \pm .4$, $C/A = 3.7 \pm .7$. The shaded area gives the distribution of events after the $N^{*++}(1238)$ isobar has been removed. It is clear from examining this figure that the major part of the asymmetry comes from the overlap of the two resonances. We therefore feel that in the present data neither interference with s- and d-waves nor the existence of a scalar meson need be invoked to explain the asymmetry.

The next question we would like to pose concerns the N^{*++} isobar. If directly produced in the primary collision it would be formed together with a pair of negative pions (see Fig. 4b). For the events produced with small momentum transfer to the $(p\pi^+)$ system, we expect the single pion exchange to dominate. We have made two tests to check for single pion exchange: (a) the πp scattering angle in $(p\pi^+)$ center of mass which should follow a $1 + 3 \cos^2\alpha$ distribution, and (b) the Treiman-Yang angle which is expected to be isotropic. Figs. 6 and 8 show the two distributions. The distribution in the scattering angle shows considerable interference effects while the Treiman-Yang angle is consistent with being isotropic. To examine interference effects with the ρ meson we looked at the distribution including and excluding events (see shaded area in Figs. 6 and 8) in the N^{*++}-ρ overlap region. The evidence for an aligned N^{*++} isobar is thus inconclusive. For comparison we show in Fig. 7 the decay angular distribution for the events with N^{*o} isobar formation. The data here are consistent with $1 + 3 \cos^2\alpha$.

One further diagram that may possibly contribute to the reaction under discussion is given in Fig. 4d. To study this channel we looked at a Dalitz plot corresponding to the following three "particles", $N^{*o}(1238)$, π^+ and π^-. In Fig. 9 we show such a diagram in which we plot the square of the $(N^{*o}\pi^+)$ mass on the x axis and that of the $\pi^+\pi^-$ mass on the y axis. A clear band corresponding to a mass of 1400-1640 MeV is seen crossing the ρ^o band. A projection of the $M^2(N^{*o}\pi^+)$ axis shows a marked peak at a mass value $M(p\pi^+\pi^-)$ = 1520 MeV and Γ = 240 MeV. The shaded area shows the events outside the ρ^o band. If we now investigate the structure of the three-particle mass peak we find that the proton forming the N^{*o} forms a $p\pi^+$ mass which lies in the $N^{*++}(1238)$ mass region (see Fig. 10). In Fig. 11 we show a Chew-Low plot of the $N^{*o}\pi^+$ events. A strong clustering of events at low four-momentum transfer to the three-particle system is evident, indicating peripheral production of the mass peak. Here we must note that at the lower vertex in Fig. 4d we can form a nucleon isobar in T = 1/2, 3/2, and 5/2 states. While the observed peak is centered at the location of the $N^*_{1/2}(1510)$ it is considerably broader than the accepted value for that isobar. We suspect that other states such as the shoulder in the T = 3/2 state may also contribute to the peak. The asymmetry in the ρ^o can now be understood to arise in part from the overlap of the ρ^o with the three-particle state which in turn decays to the N^{*++} isobar. We must further note that another possible origin for the observed mass peak may be interference effects between diagrams 4a and 4b taking into account the Bose symmetrization of the two negative pions.[3]

Finally, we would like to discuss the properties of the two identical bosons, $\pi^-\pi^-$. The most surprising feature is the distribution in the $\pi^-\pi^-$ scattering angle (see Fig. 12). The distribution has all the earmarks of an aligned high angular momentum state. We cannot find, however, any particular mass enhancement associated with the angular distribution. In a study of a correlation between the $N^{*o}\pi^+$ mass and the $\pi^-\pi^-$ scattering angle we find the above mass peak is directly related to the anisotropy in the scattering angle. The anisotropy may thus be due in part to the observed mass peak, although the presence of T = 2 d-wave scattering in the $\pi^-\pi^-$ system cannot be ruled out. The symmetry in the distribution shown arises from the fact that the two negative pions are indistinguishable.

REFERENCES

1. G. Puppi, Annual Review of Nuclear Science, Vol. 13, p. 287 (Annual Reviews, Inc., Palo Alto, California 1963), Editor, E. Segre.

Saclay-Orsay-Bari-Bologna Collaboration, Nuovo Cimento 29, 515 (1962).

V. Hagopian and W. Selove, Proceedings of the Athens Conference on Recently Discovered Particles, p. 270, Ohio University Press, Athens, Ohio, 1963.

2. P. Bareyre, C. Bricman, G. Valladas, G. Villet, J. Blizard, J. Seguinot, Phys. Letters 8, 137 (1964). Extensive compilation of total cross sections and inelastic cross sections up to 700 MeV.

J. A. Helland, C. D. Wood, T. J. Devlin, D. E. Hagge, M. J. Longo, B. J. Moyer, and V. Perez-Mendez, "Elastic Scattering of Negative Pions on Protons in the Energy Range 500 to 1000 MeV", Phys. Rev. (to be published).

3. We have greatly benefited from discussions with Professor F. Low on this subject.

FIGURE CAPTIONS

Fig. 1. Mass distributions of the two-particle $(\pi^-\pi^+)$, $(p\pi^+)$ and $(p\pi^-)$states.

Fig. 2. Mass distributions of $(p\pi^-)$ state formed in the reaction

$\pi^- + p \rightarrow \rho^0 + p\pi^-$

Fig. 3. Scatter diagram of $(\pi^+\pi^-)$ mass versus $p\pi^+$ mass.

Fig. 4. Feynman diagrams for reactions

(a) $\pi^- + p \rightarrow \rho^0 + N^{*0}$

(b) $\pi^- + p \rightarrow \pi^- + \pi^- + N^{*++}$

(c) $\pi^- + p \rightarrow A^- + p$

(d) $\pi^- + p \rightarrow \pi^- + N^{*0}\pi^+$

Fig. 5. Distribution in $\pi^-\pi^-$ scattering angle in ρ^0 center of mass.

Fig. 6. Distribution in $p\pi^+$ scattering angle in $p\pi^+$ center of mass.

Fig. 7. Distribution in $p\pi^-$ scattering angle in $p\pi^-$ center of mass.

Fig. 8. Treiman-Yang angle computed at N^{*++} vertex.

Fig. 9. Dalitz plot of $M^2(N^*\pi^+)$ versus $\pi^+\pi^-$ with respective projections.

Fig. 10. Chew-Low plot of $M^2(N^{*0}\pi^+)$.

Fig. 11. Invariant mass distribution of $p\pi^+$ for events in mass peak $1400 < M(N^{*0}\pi^+) < 1640$ MeV.

Fig. 12. Distribution in $\pi^-\pi^-$ scattering angle.

Table I. Cross sections for the various channels in the reaction

$$\pi^- + p \longrightarrow \pi^+ + \pi^- + p + \pi^-$$

Channel	Events		Cross Section[a] mb	
1. $\rho^0 + N^{*0}(1238)$	50	140	0.085 ± .025	0.24 ± .07
$\rho^0 + N^{*0}(1510)$	44		0.075 ± .025	
$\rho^0 + N^{*0}(1688)$	46		0.078 ± .025	
2. $\rho^0\pi^-p$ → A^-p	160[b]	290	0.27 ± .08[b]	0.50 ± .15
$\rho^0\pi^-p$ → $\rho^0\pi^-p$	130		0.23 ± .07	
3. $N^{*++}\pi^-\pi^-$ → $(p\pi^+\pi^-)\pi^-$	90	260	0.15 ± .05	0.44 ± .11
$N^{*++}\pi^-\pi^-$ → $N^{*++}\pi^-\pi^-$	170		0.29 ± .10	
4. $N^{*0}(1238)\pi^+\pi^-$, $\pi^+\pi^-p\pi^-$	340		0.60 ± .2	
TOTAL	1030		1.8 ± 0.4	

(a) all cross sections have been normalized to the total π^-p cross section.

(b) the events in the A_1 and A_2 regions are included here.

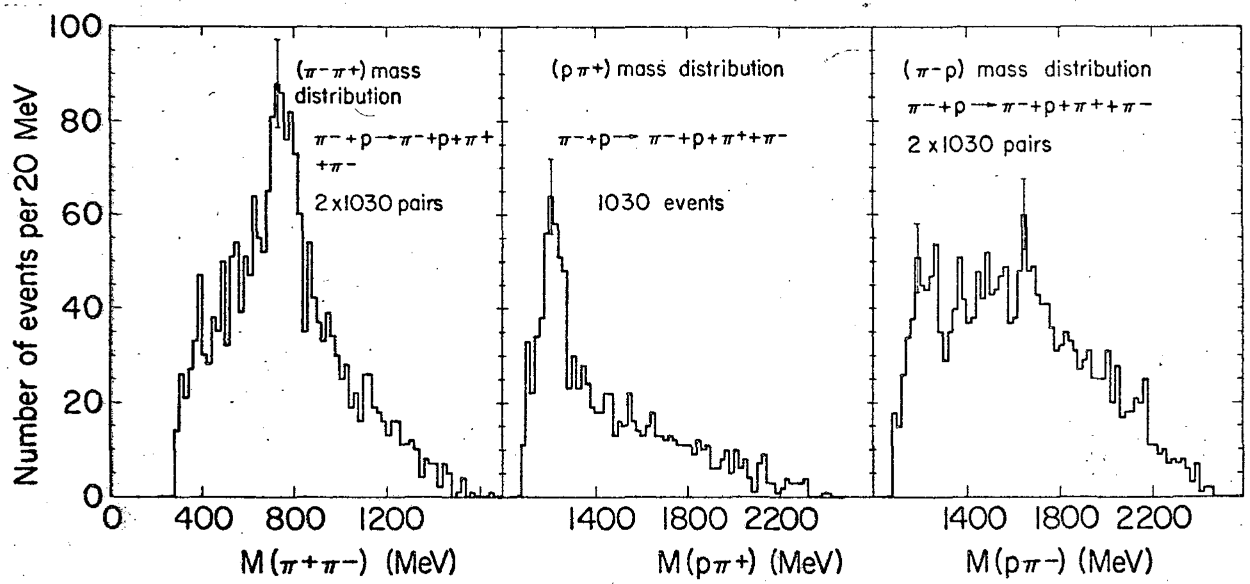

Number of events per 20 MeV
100
80
60
40
20
0
(π−π+) mass distribution
π− + p → π− + p + π+ + π−
2 x 1030 pairs
0
400
800
1200
M(π+π−) (MeV)
(pπ+) mass distribution
π− + p → π− + p + π+ + π−
1030 events
1400
1800
2200
M(pπ+) (MeV)
(π−p) mass distribution
π− + p → π− + p + π+ + π−
2 x 1030 pairs
1400
1800
2200
M(pπ−) (MeV)

Figure 1

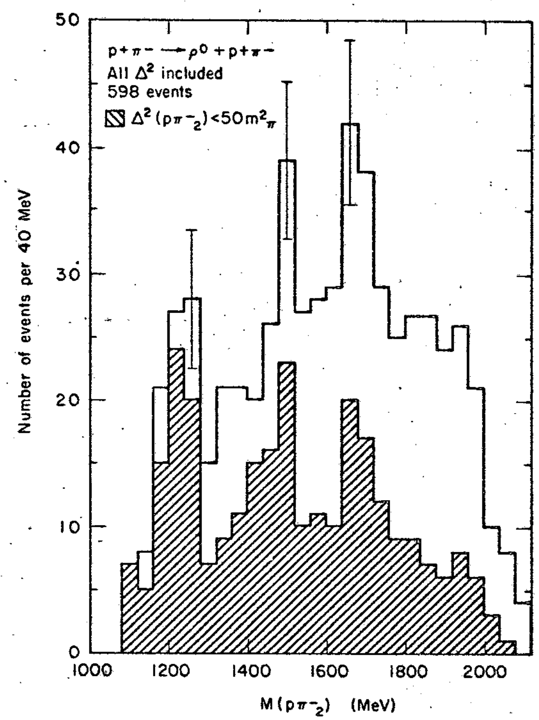

Figure 2

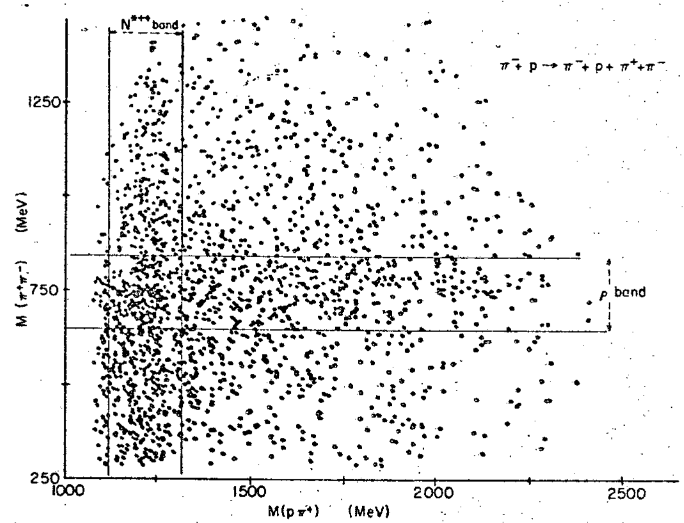

Figure 3

MUB-3447

Figure 4

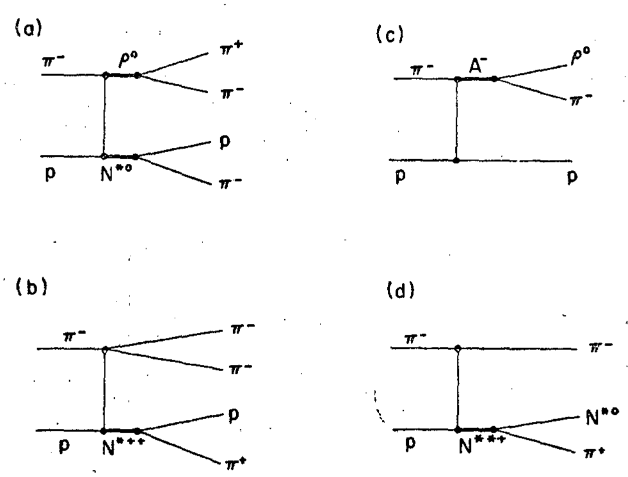

Figure 5

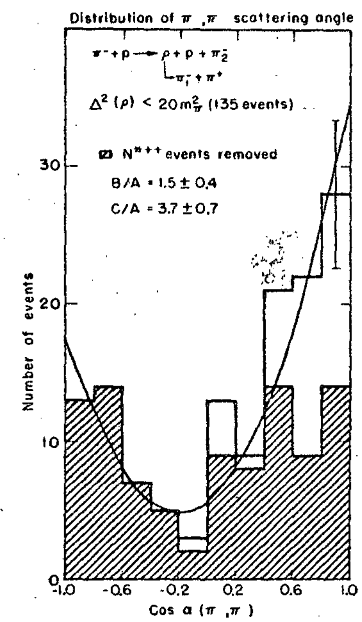

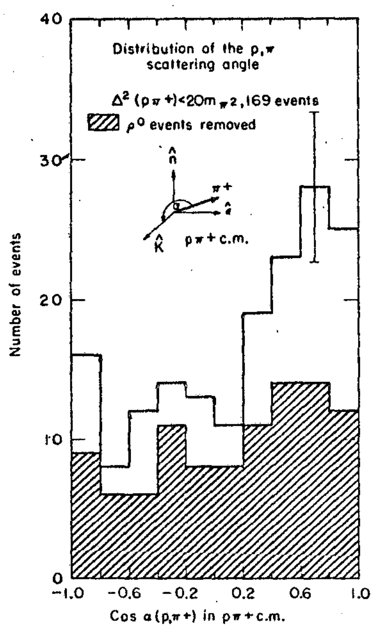

Figure 6

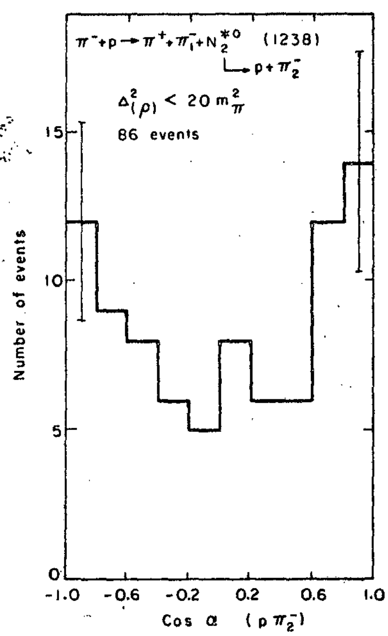

Figure 7

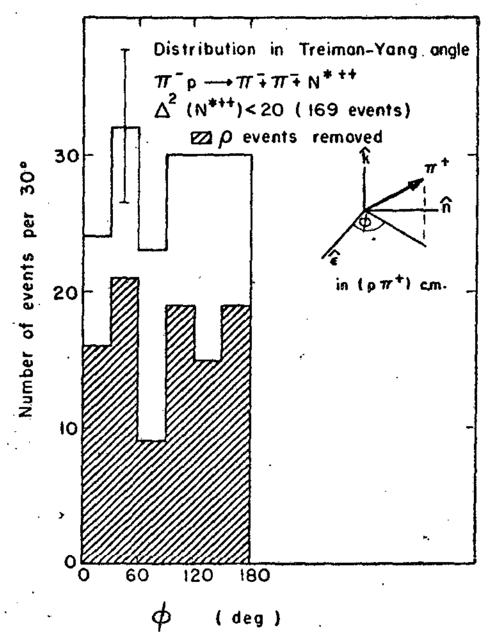

Figure 8

MUB-3448

Figure 9

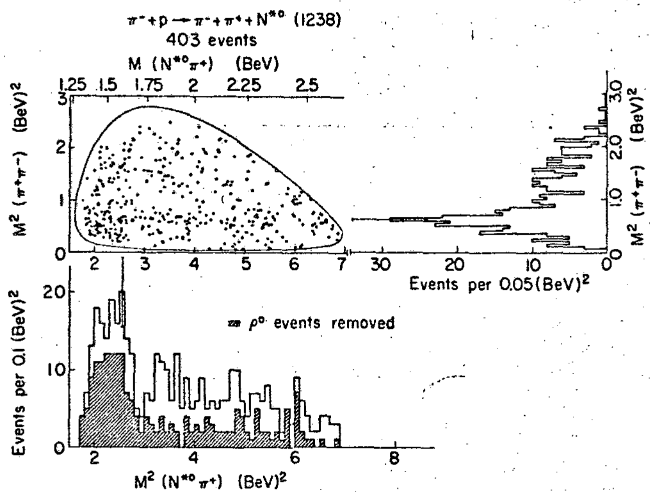

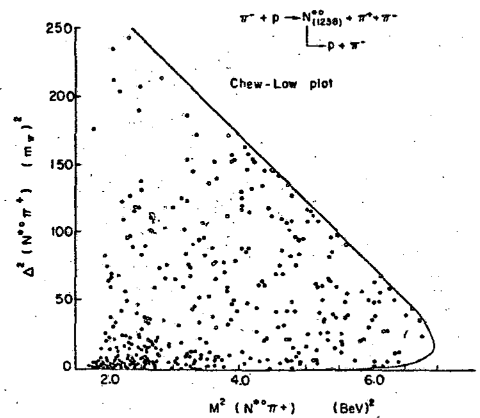

Figure 10

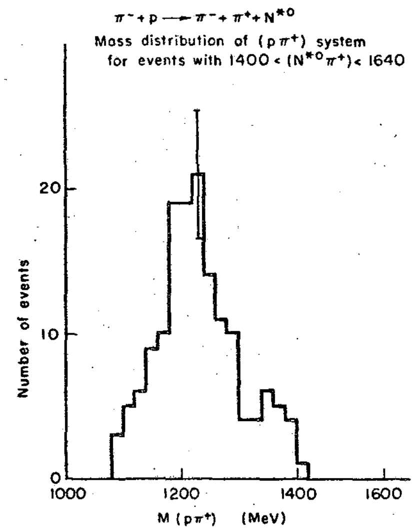

Figure 11

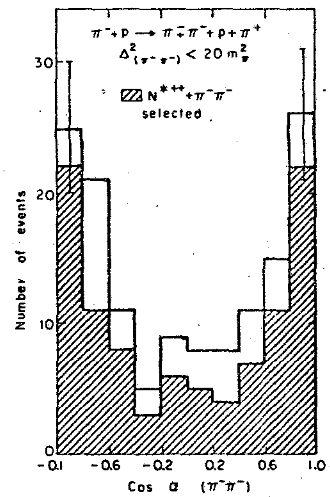

Figure 12

MUB-3449